This is a peer-reviewed, accepted author manuscript of the following conference paper: Habibi, P, Algaddaime, TF, Lotfian, S & Stack, MM 2024, 'Investigating the effect of erosion induced surface roughness on tidal turbine blade performance: part 1', Paper presented at the Tenth International Conference on Engineering Failure Analysis, Athens, 7/07/24 - 10/07/24.

Investigating the Effects of Erosion-Induced Surface Roughness on Tidal Turbine Blade Performance - Part I

Payvand Habibi*; Talal F. Algaddaime; Saeid Lotfian* and Margaret M. Stack****

* payvand.habibi@strath.ac.uk; saeid.lotfian@strath.ac.uk; Naval Architecture, Ocean and Marine Engineering (NAOME) - University of Strathclyde – Glasgow - G1 1XQ

** Talal.algaddaime@strath.ac.uk (T.F.A); margaret.stack@strath.ac.uk (M.M.S)); Mechanical and Aerospace Engineering - University of Strathclyde – Glasgow - G1 1XQ

Abstract

The renewable energy sector develops the most outstanding engineering ideas and brings them into action to mitigate further environmental damage. Yet, some failure mechanisms concerning causes, effects, and solutions must be studied. This study explores erosion as one of the most problematic phenomena in tidal turbine blades. This failure first targets structural integrity on the blade surface and gradually propagates to the substrate. Erosion can trigger failures like fatigue, corrosion, and ageing. These failures can also make erosion worse. Eventually, this wear leads to tribological breakdown and hydrodynamic failure even before the design lifetime ends. Erosion starts with pits on the blade's leading edge and gradually grows, penetrates and spreads all over the blade. Before the complete delamination, the turbine keeps serving despite a considerable reduction in its performance due to a rough blade surface. The relation between erosion-induced roughness and performance reduction is still unknown. Apart from a lack of industrial cases, the existent prototypes have been commissioned quite recently. In addition, the exclusive effect of erosion on the turbine performance cannot be evaluated from a real turbine because of the impact of other failures. Therefore, a parametric study has been carried out to investigate the influence of erosion on the tidal turbine blade surface. Implementing a range of roughness heights from 0.01mm to 1.2 mm on the blade section at Reynold's number of 1.6e+6, the effect of early-stage erosion severity on the hydrofoil efficiency is investigated. The effect of erosion on the fibre-reinforced polymer surface for different impact angles and periods has also been experimentally studied. This was through erosion tests on glass fibre-reinforced polymer plates (FR4) in a sand-salt-water erosion rig. As the results show, the severity of erosion increases over time. Furthermore, erosion increases with impingement angles up to 60 degrees and then decreases at 90 degrees. These outcomes will lead us to the next step, investigating the impact of erosion on the efficiency of the tidal turbine blade. This paper is part one of a two-part study. In part II, the influence of erosion-induced roughness distribution on the hydrofoil efficiency is numerically studied.

Keywords:

Tidal turbine; Structural integrity; Failure; Roughness; Performance; Efficiency.

Introduction

Global warming and the finite fossil fuel resources led us to renewable energies to reduce carbon emissions (Sangiuliano, 2017;Qian et al., 2019). This means transitioning from fossil fuels to other energy sources like hydroelectricity, solar, and wind, which are now important sectors that can vastly tabernacle oil and gas. Solar and wind energy converters are the most used types, and hydroelectricity generators are expanding steadily (Clark and DuPont, 2018;Neill, 2018). Even though the oceans cover more than 70% of the globe, the hydroelectricity's share of total generated renewable energy is not considerable. This might be due to environmental constraints. Marine renewable energy resources contain offshore winds, waves, tidal currents, and ocean thermal and salinity gradients (Jing et al., 2017). Offshore winds and tidal currents have the most promising kinetic energy to be converted into electricity (Qian et al., 2019). The cyclic gravitational forces of orbiting celestial bodies drive tidal currents in two-directional cycles (Izadi Gonabadi, 2019). The greater density of water, around 850 times higher than air, results in tidal turbines generating more thrust and power than wind turbines of the same capacity. Tidal flow velocities can reach up to 2.5 m/s in narrow passages around islands and cliffs, making them an invaluable energy source (Finkl and Charlier, 2009). Tidal current converters also benefit from precise predictability based on astronomical tidal cycles, giving them an advantage over variable wind and solar resources (Zhou et al., 2017). Various methods have been suggested to utilise tidal currents, such as horizontal axis (h-axis) turbines, vertical axis (v-axis) turbines, oscillating hydrofoils, and venturi effect devices (Khan et al., 2009;Neill, 2018). H-axis tidal turbines are similar to wind turbines and are currently the most advanced and commercially viable technology (Arcos, 2021). They benefit from the buoyancy force to balance the weight force effectively (Jing et al., 2017). Tidal turbines, on the other hand, experience torque loads that are 50% higher than wind turbines. This means their structural designs must be more robust to sustain their operations in the harsh marine environment for 20-25 years (Song et al., 2020). The materials and components used for tidal blades must endure constant load reversals, corrosion, cavitation, and erosion. The development process for energy converters, such as wind turbines and tidal devices, takes decades. This is primarily due to the requirement for dependable and effective technologies that can withstand severe operational environments (Wood et al., 2010).

Operating in remote offshore locations and durability in harsh marine environments are significant challenges. Erosion is one of the most common phenomena underwater due to suspended particles and fluid flow around the turbine blade. By reducing the blade's structural integrity, erosion creates roughness on the turbine blade's surface. In this study, a numerical parametric analysis is conducted, and it shows that erosion-induced roughness will decrease the tidal turbine's performance. The following articles provide detailed information about this parametric study.

Investigating the blade surface's response to erosion is the first step towards understanding its structural and hydrodynamic behaviour in real operational conditions. This research observes the sand erosion and consequent mass loss of FR4 samples (as a highly likely Glass-Fiber Reinforced Composite used in the tidal turbine industry). A series of tests were conducted in an in-house sand-salt-water erosion rig for different impingement angles but the same sand size and concentration. The details of the experiments and the methodology are provided in the next parts.

Methodology

Numerical Study

To investigate the effect of erosion-induced roughness on the tidal turbine performance, a parametric study is carried out on a NACA 65-475 at Reynold's (Re) number of 1.6e+6 and an angle of attack (AOA) equal to zero. Mesh study through the validation process led to y+<1 for smooth and 30<y+<300 for rough blade surface.

A smooth (intact) blade section simulation is validated with the experiments conducted by Bak et al. (Bak *et al.*, 2000). We used a powerful computational fluid dynamic (CFD) tool named Star CCM+ to simulate and analyse the problem. Steady-state Reynolds Average Navier Stokes (RANS), K-ω SST turbulence model is applied on a NACA 63-415 hydrofoil at Re=1.6e+6, with AOA of 0, 2.5, 5, 7.5, and 10 degrees. The lift-to-drag coefficient, known as hydrodynamic efficiency, is a parameter to validate the results. Figure 1 to Figure 4 show details of the mesh and the flow velocity field of the validated simulation at Re=1.6e+6 and AOA=0. The numerical results compared to the reference validating experimental outputs are illustrated in Table 1.

Table 1 Numerical simulation of smooth NACA 63-415 at Re=1.6e+6

Angle of Attack (deg)	Numerical Simulation (current study)		Experiments by Bak et al.	CFD/Experiment Error (%)
	Y+ < 1	Cl/Cd	Cl/Cd	Cl/Cd
0	Y	3.23E+01	3.19E+01	1.2
2.5	Y	5.47E+01	5.79E+01	5.7
5	Y	6.71E+01	6.87E+01	2.5
7.5	Y	6.93E+01	7.13E+01	2.9
10	Y	6.39E+01	6.50E+01	1.7

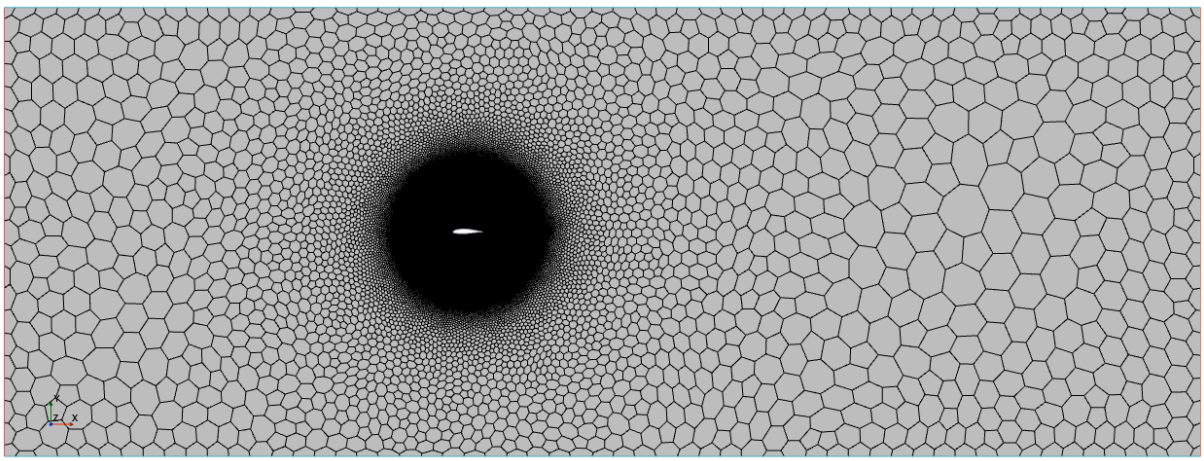

Figure 1 The generated mesh domain to validate the numerical outputs with y+<1 for smooth NACA 63-415 section.

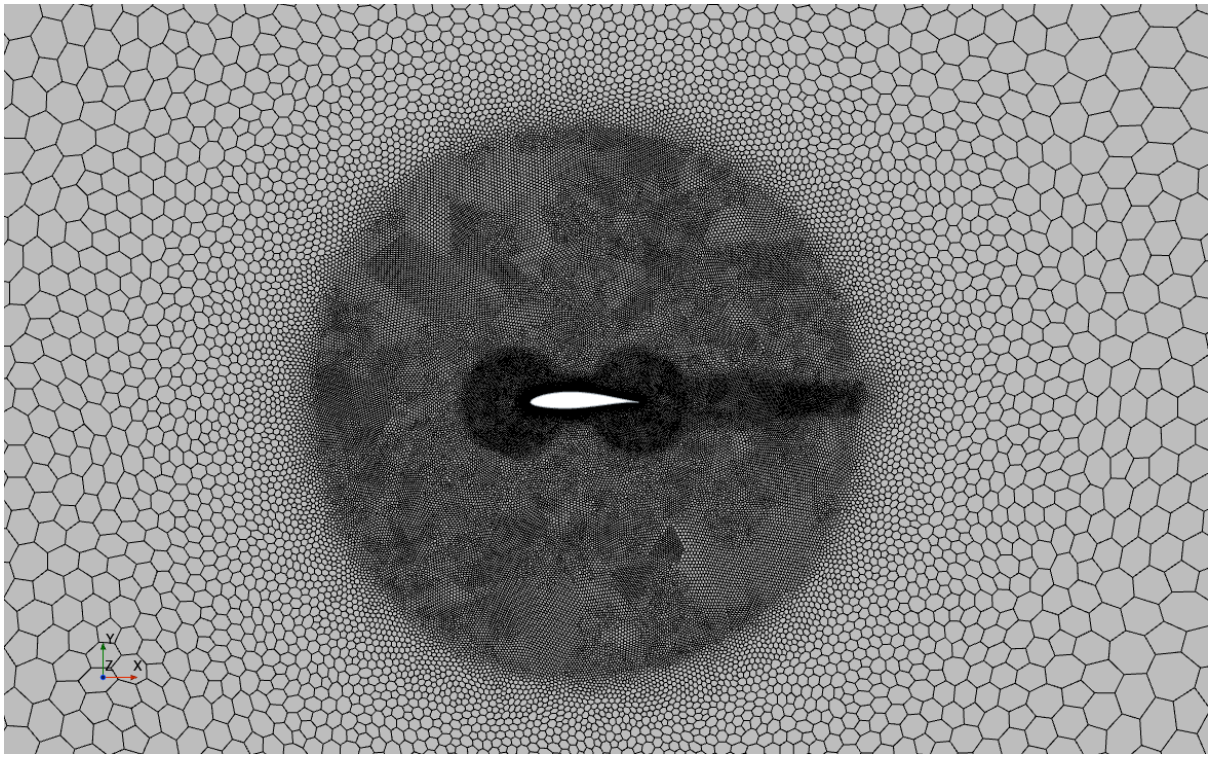

Figure 2 The mesh volumetric control for smooth NACA 63-415 section with y+<1 from a closer view.

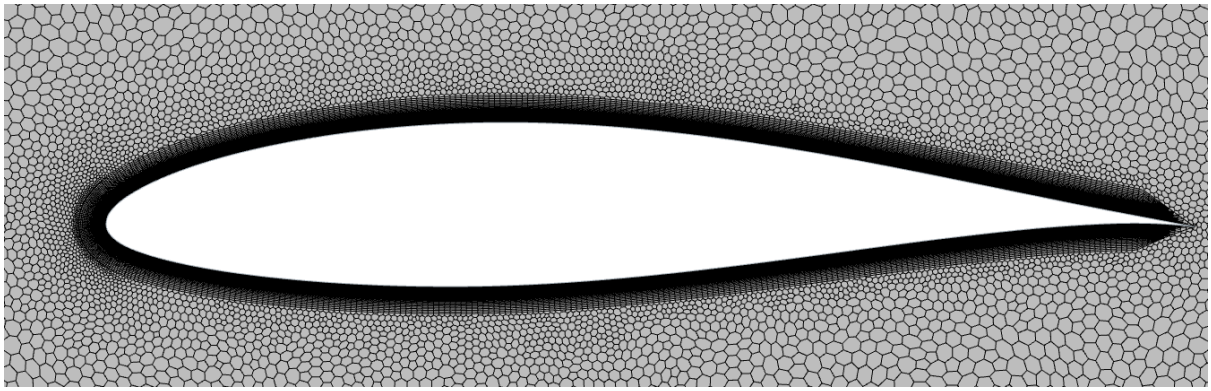

Figure 3 The prism layer mesh for smooth NACA 63-415 section with y+<1 from a closer view.

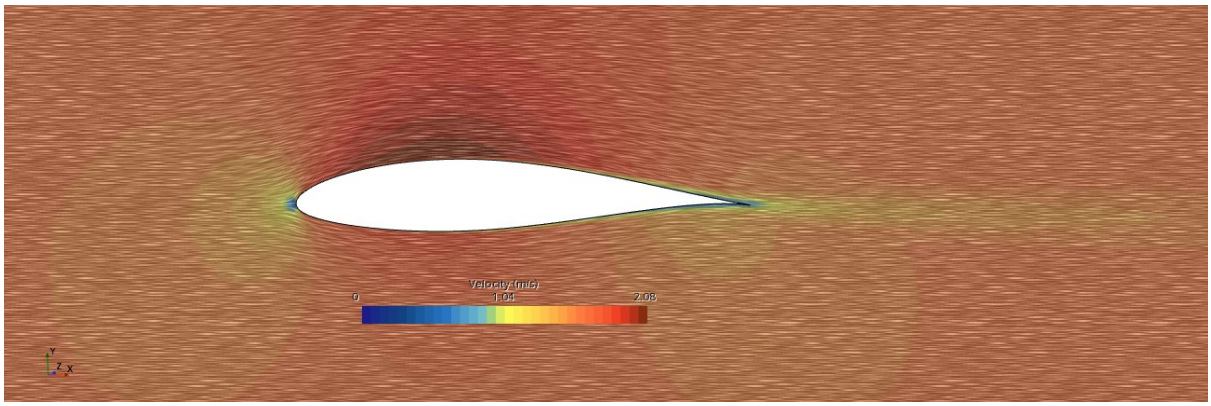

Figure 4 Flow velocity field around NACA 63-415 at Re=1.6e+6, and AOA=0.

Experimental Tests

Slurry Erosion Impingement Rig

According to the literature reviews, slurry erosion was first recognised as an issue in the oil and munitions sectors during World War II. The industrial components suffered extensive damage due to their contact with fluid and particle inclusion, resulting in significant financial losses. Hence, scientists have developed various slurry erosion test sets, and each set is labelled after the initial test set-up designers. The Levy, Hutchings, Turenne, and Thapa test methods are the most common slurry erosion (Karthik and Amarendra, 2020).

In this study, a slurry erosion rig was developed at the University of Strathclyde in the tribology laboratory to artificially reproduce tidal turbine blades to examine Glass-Fiber-Reinforced Polymer (GFRP) and meet the experiment's purpose, which is to investigate erosion in the harsh marine environment. Figure 5 shows the slurry erosion impingement rig.

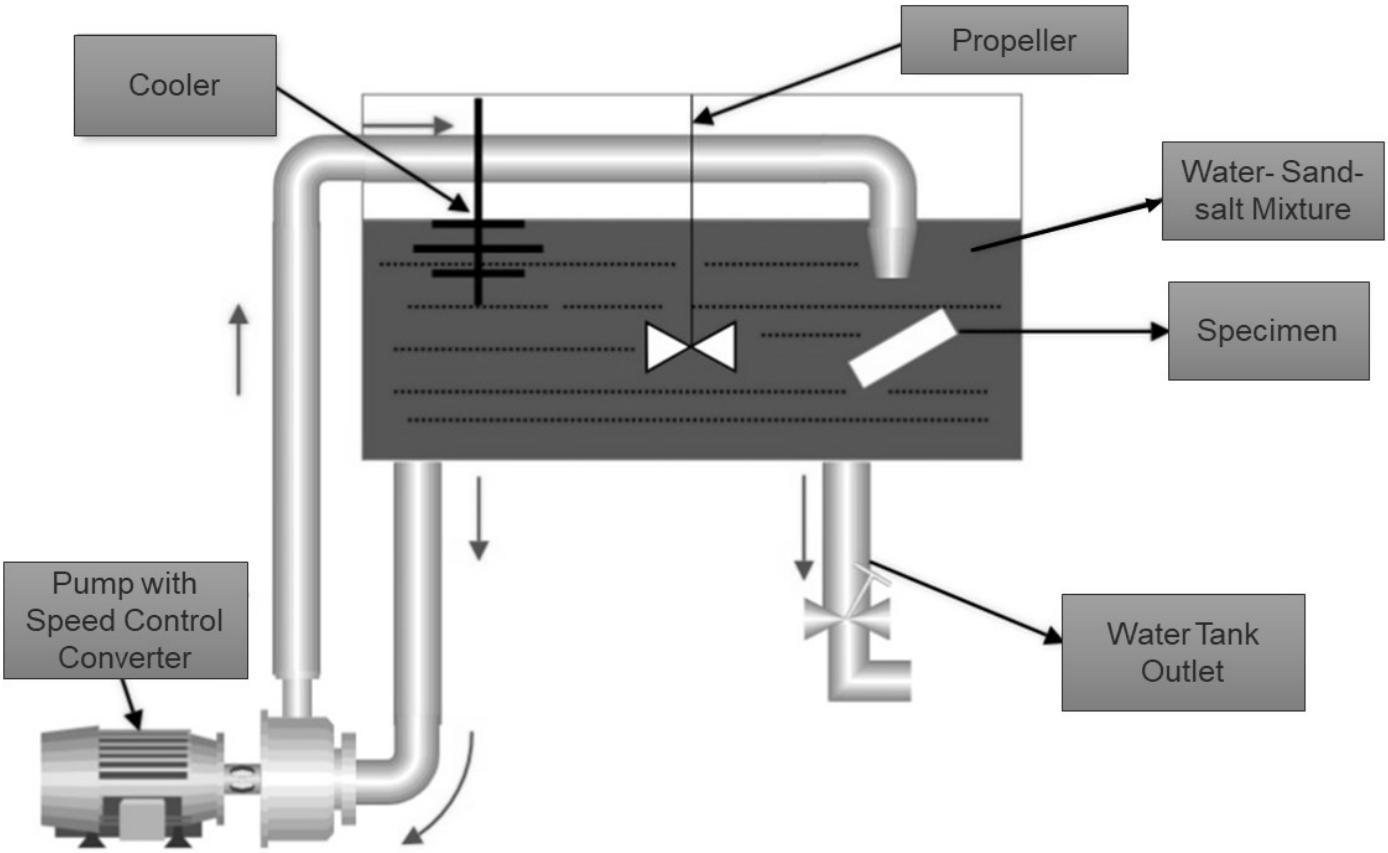

Figure 5 Schematic Diagram of Slurry Erosion Impingement Rig

The variables for this examination are the effectitve velocity under different impact angle at 30°, 45°,60°, and 90 °, to investigate erosion behaviour. In addition, the GFRP was exposed to water for two weeks to investigate material ageing. The examination was then performed in three different time durations: 30, 60, and 90 minutes. Table 2 shows the parameters used in this study. Each test with the following characteristics is repeated on at least three new samples, and the final results are declared based on the average output in each test scenario.

Table 2 Erosion Test Parameters.

Parameter	Value
Impingement angle	30°, 45°, 60°, 90°
Solution	Water, Salt, and Sand
Water tank capacity (Liter)	13 litters
Salinity (wt %)	3.5%
Sand concentration (wt%)	3%
Test duration (min)	30, 60 and 90mins
Sand Particle Size (μm)	100 - 150μm
Temperature	10℃ ±1℃
Impact velocity (ms-1)	12.5m/s

Material selection:

The FR4 material selected in the experiment as a specimen is constructed from a woven glass fabric combined with a high-strength epoxy resin. When choosing a material for a specific use, its characteristics must meet the requirements of the purpose of the components, the conditions in which it will be used, or the intended structure. Several variables influence the choice of material for tidal current turbines and may be stated as component shape; dimensional tolerance required; mechanical properties such as strength, stiffness, hardness, and fatigue strength; chemical properties like corrosion properties; physical properties such as density; life cycle costs like cost of material, cost of manufacture, cost of maintenance and cost of installation and removal (Shiekh Elsouk, Santa Cruz and Guillou, 2018).

Glass fibre-reinforced polymer (GFRP) is frequently used in constructing turbine blades due to its ability to combine the necessary structural stiffness for big constructions with the lightweight properties required for complicated geometries (Groucott *et al.*, 2021). Hence, according to the Holbourne Industrial Plastics Ltd data sheet, the material is formulated to have good mechanical strength and excellent electrical properties combined with a high impact and humidity resistance at continuous operating temperatures of up to 130°C. The mechanical properties of GFRP are provided in Table 3. The specimen's dimensions were 25 mm × 35 mm, and thickness was 5 mm.

Table 3 Technical Data, Mechanical and Electrical Properties of GFRP-FR4.

Technical Data	Units	Test Method	Values
Colour	-	-	Light Green
Specific Gravity	g/cm³	ISO 1183	1.95
Water Absorption	mg	ISO 62	5.5
Temperature Index	-	IEC 60216	130°C
Mechanical Properties			
Flexural Strength	MPa	ISO 178	500
Compressive Strength	MPa	ISO 604	-
Impact Strength Charpy	kJ/M ²	ISO 179	60
Tensile Strength	MPa	ISO 527	450
Electrical Properties			
Insulation Resistance	MΩ	IEC 60893	1.0 x 10^9
Breakdown Voltage	kV	IEC 60243	42
Dielectric Strength	kV/mm	IEC 60243	24

Mass measurements:

The primary method for recording erosion was to measure the mass loss of each specimen before and after the test. The BM252 micro-analytical balances with a repeatability (standard deviation) of about 0.03 mg (for 100 g) was adopted to make the measurement. This allowed for direct comparison between each test and provided data detailing the impact angles and velocity to erosion for the FR4 Epoxy Glass fibre material. Figure 6 The A&D BM252 Micro Analytical Balances illustrates the micro-analytical balances A&D-BM252. .

Figure 6 The A&D BM252 Micro Analytical Balances

Results

Numerical Study:

Having the validated settings for the smooth blade simulation, the mesh is modified to meet the required y+ between 30 and 300 for rough surfaces to capture the effect of roughness height on the hydrodynamic efficiency. The lift and drag coefficients are calculated for the NACA 63-415 at Re=1.6e+6, AOA=0, with surface roughness heights of 0, 0.01, 0.02, 0.05, 0.1, 0.2, 0.25, 0.3, 0.5, 0.7, 0.8, 1.0, 1.2 mm. The changes in lift and drag coefficients and the corresponding efficiency reduction are tabulated in Table 4.

Table 4 NACA 63-415 lift and drag coefficients and efficiency changes for a range of surface roughness heights.

Roughness Height (mm)	Efficiency Drop %	CL Drop %	CD Rise %
0.01	6.97	1.87	5.48
0.02	6.97	1.87	5.49
0.05	7.89	2.02	6.37
0.1	15.14	3.32	13.93
0.2	27.90	6.18	30.13
0.25	32.55	7.45	37.22
0.3	36.05	8.50	43.09
0.5	40.08	10.04	50.14
0.7	40.32	10.17	50.51
0.8	40.32	10.17	50.51
1	40.32	10.17	50.51
1.2	40.32	10.17	50.51

It should be noted that the upper and lower surfaces of the hydrofoil are considered fully rough with a uniform distribution. Figure 7 and Figure 8 demonstrate how drag and coefficients change while surface roughness increases. Figure 9 shows lift-to-drag (efficiency) behaviour against surface roughness.

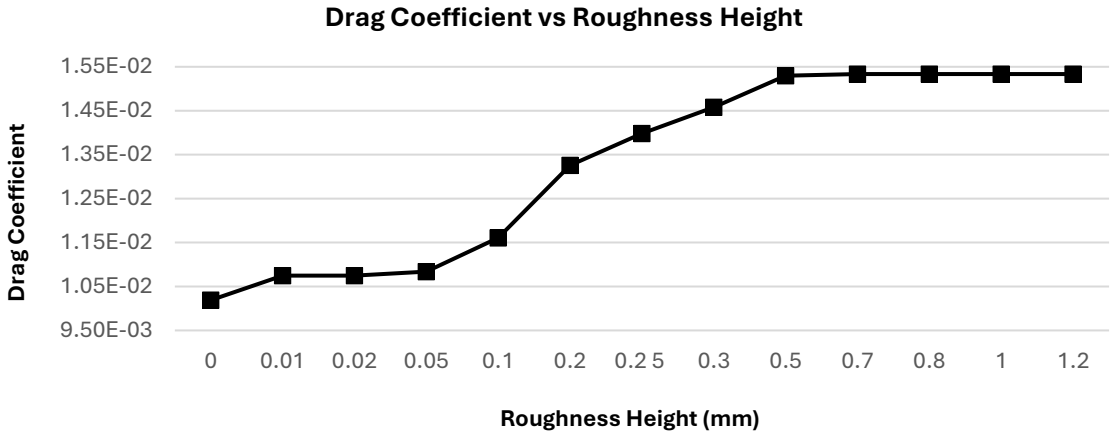

Figure 7 Drag Coefficient of NACA 63-415 at Re=1.6e+6, AOA=0, against surface roughness height.

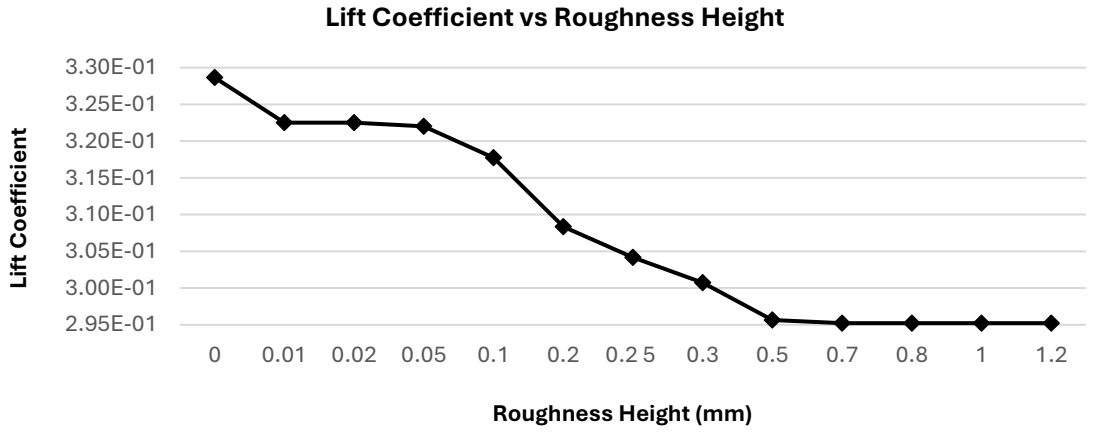

Figure 8 Lift Coefficient of NACA 63-415 at Re=1.6e+6, AOA=0, against surface roughness height.

Figure 9 Lift to Drag Coefficient (efficiency) of NACA 63-415 at Re=1.6e+6, AOA=0, against surface roughness height.

As the graphs show, roughness can decrease blade efficiency by up to 40 per cent. To investigate the effect of erosion-induced roughness on tidal turbine blade performance, the behaviour of the material considered against erosion in a sand-salt-water medium must be studied.

Experimental Study:

As mentioned in the last articles, the erosion behaviour of FR4-GFRC is observed through a set of experimental tests. The mass loss of each test case is the erosion measure. It can be seen in Figure 10 and Figure 11 that mass loss is equal to volume loss, which means the surface geometry of the target sample changes. In other words, erosion changes the external shape of the body, which is crucial in its hydrodynamic response.

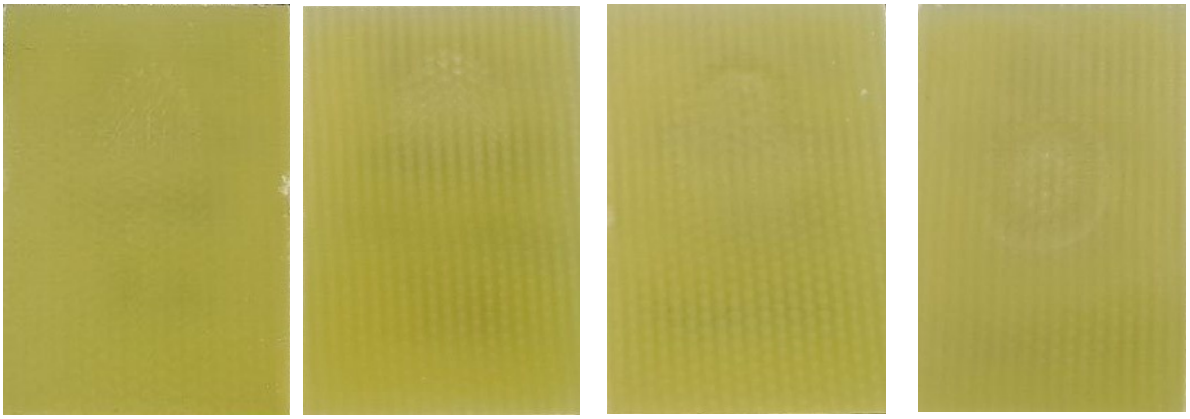

(a) (b) (c) (d)

Figure 10 Eroded FR4-GFRC samples in 90 minutes, 100 – 150μm sand size, and 12.5 m/s impingement velocity, a) 30°, b) 45° , c) 60° , and d) 90° impingement angles (with naked eyes).

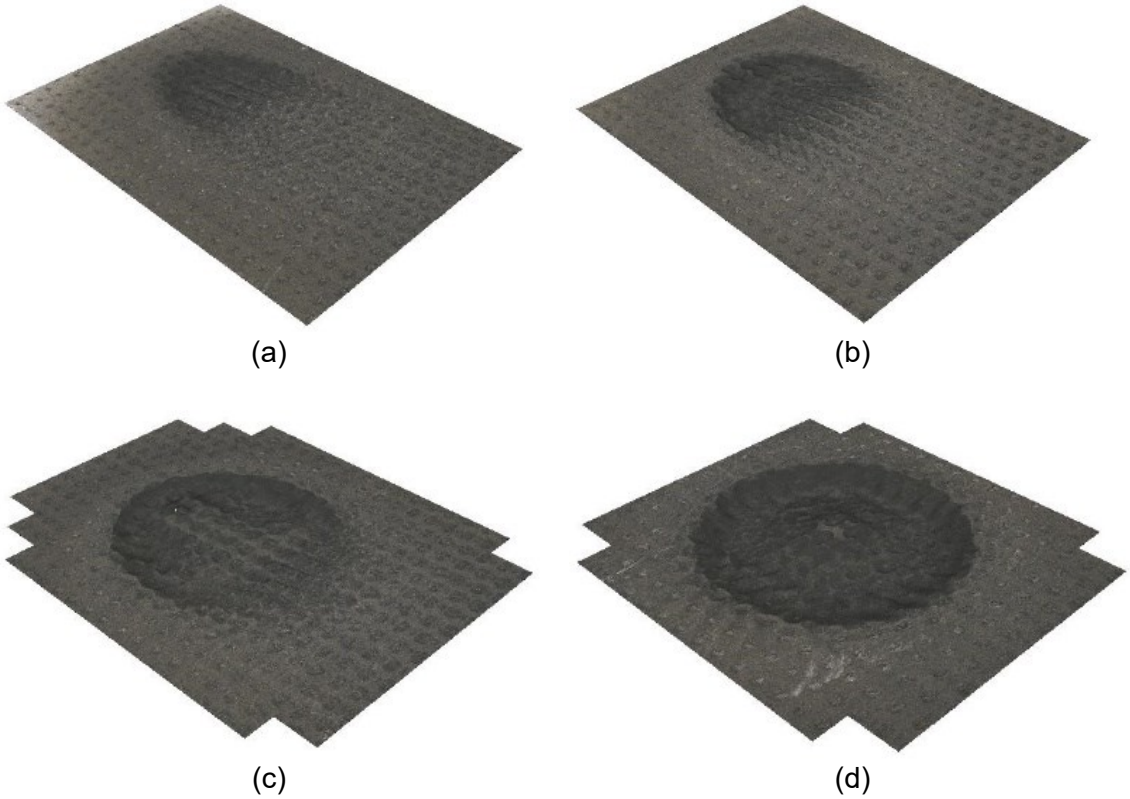

(a) (b) (c) (d)

Figure 11 Eroded FR4-GFRC samples in 90 minutes, 100 – 150μm sand size, and 12.5 m/s impingement velocity, a) 30°, b) 45° , c) 60° , and d) 90° impingement angles (3D view captured by Alicona 3D surface scanner)

Figure 12 to Figure 14 demonstrate the mass losses of tested samples in different impingement angles in 30 minutes, 60 minutes, and 90 minutes, respectively.

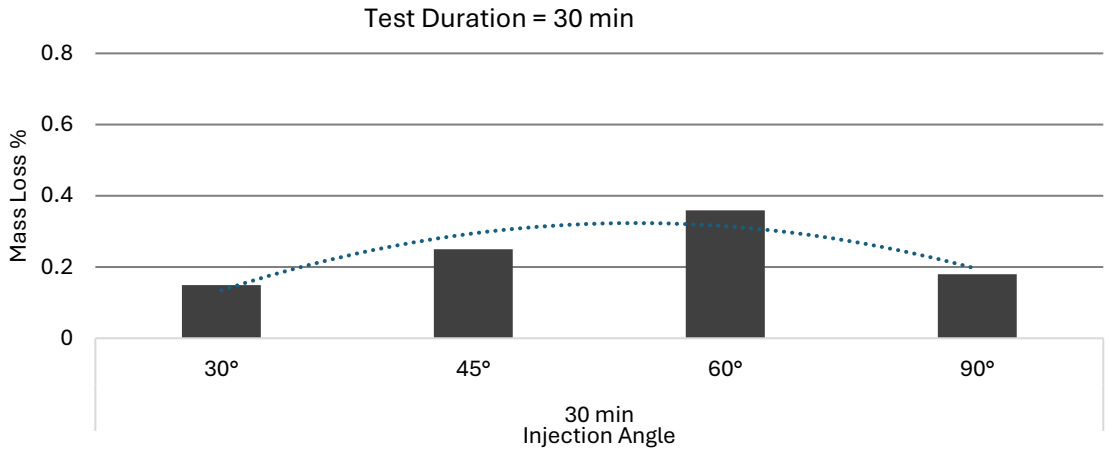

Figure 12 Erosion-induced mass loss of FR4-GFRC sample in different impingement angles in 30 minutes, 100 – 150μm sand size, and 12.5 m/s impingement velocity.

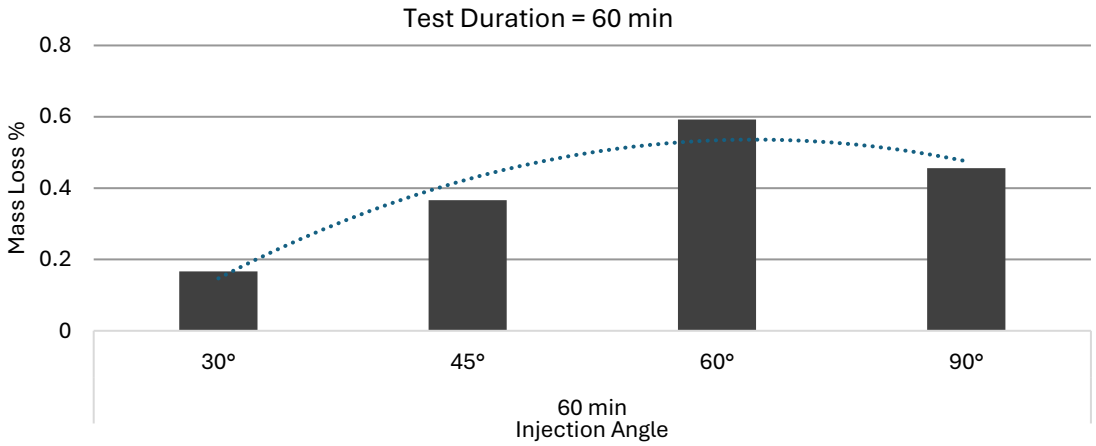

Figure 13 Erosion-induced mass loss of FR4-GFRC sample in different impingement angles in 60 minutes, 100 – 150μm sand size, and 12.5 m/s impingement velocity.

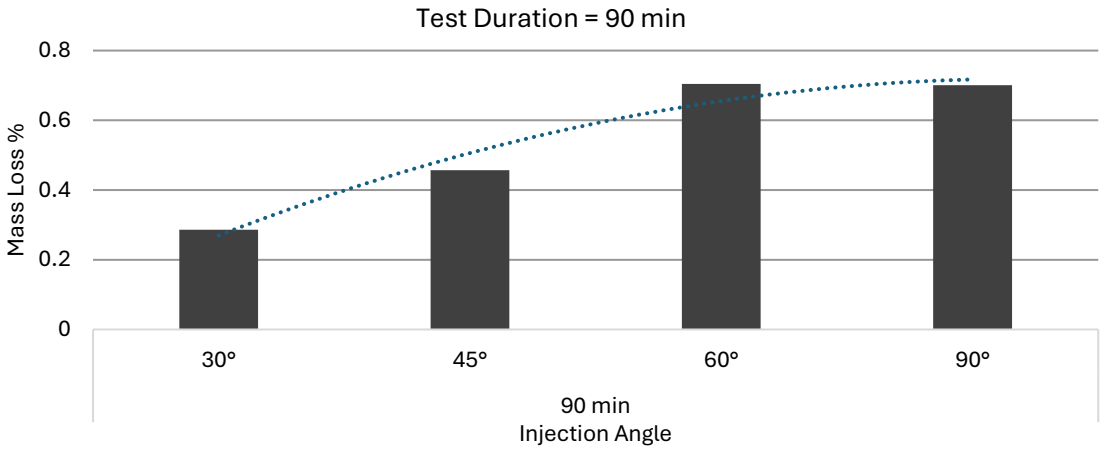

Figure 14 Erosion-induced mass loss of FR4-GFRC sample in different impingement angles in 90 minutes, 100 – 150μm sand size, and 12.5 m/s impingement velocity.

According to these graphs, the maximum mass loss happens at the impingement angle of $60°$, while the minimum mass loss is observed at the impingement angle of $30°$.

Figure 15 to Figure 18 display another interpretation of experimental outputs. The mass losses of samples in each impingement angle are compared for different test durations. In other words, the effect of exposure time on erosion (mass loss) is explored. According to the reported mass loss, as was expected in each test scenario, the erosion increases over time. So, the logical conclusion is that erosion-induced volume loss (shape change) increases over time. This, in addition to the results of the parametric study, means that the tidal turbine efficiency will drop over time while confronting erosion.

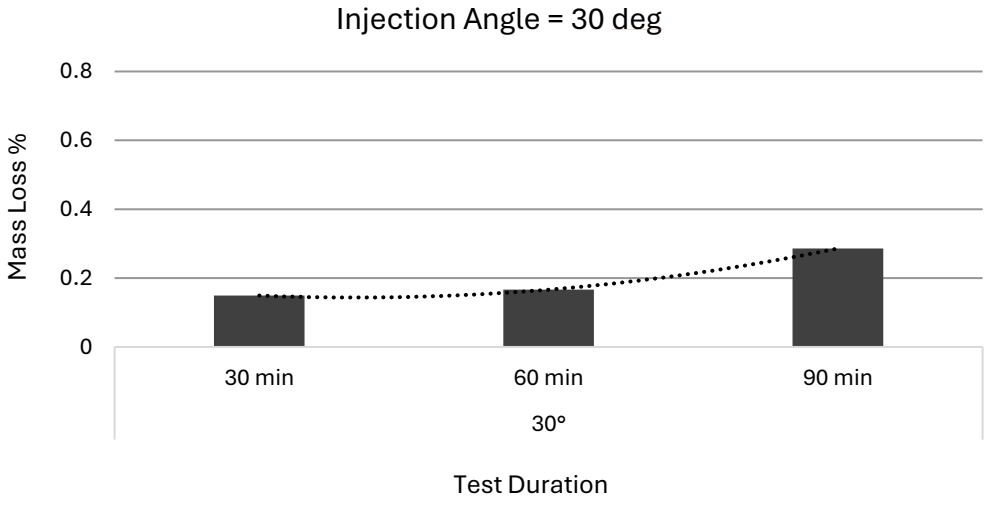

Figure 15 Erosion-induced mass loss of FR4-GFRC sample in different test durations, $30°$ impingement angle, 100 – 150μm sand size, and 12.5 m/s impingement velocity.

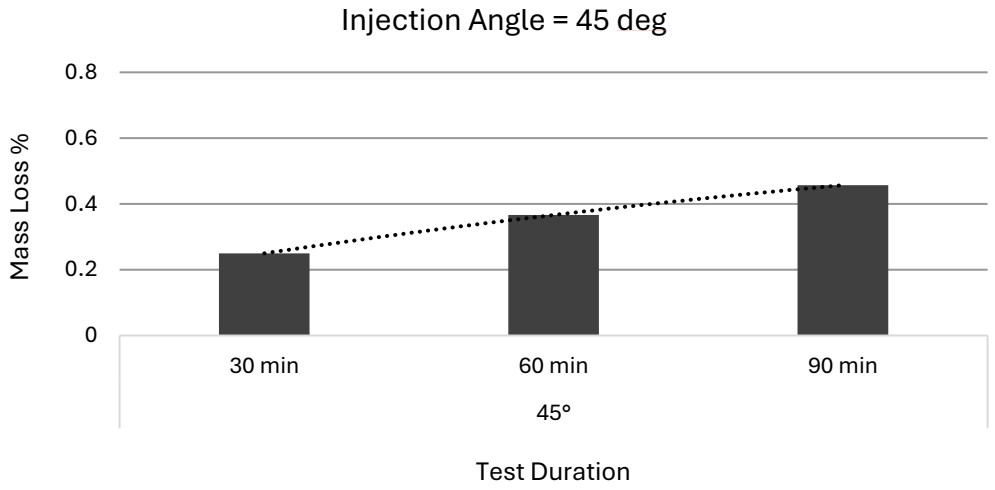

Figure 16 Erosion-induced mass loss of FR4-GFRC sample in different test durations, 60° impingement angle, 100 – 150µm sand size, and 12.5 m/s impingement velocity.

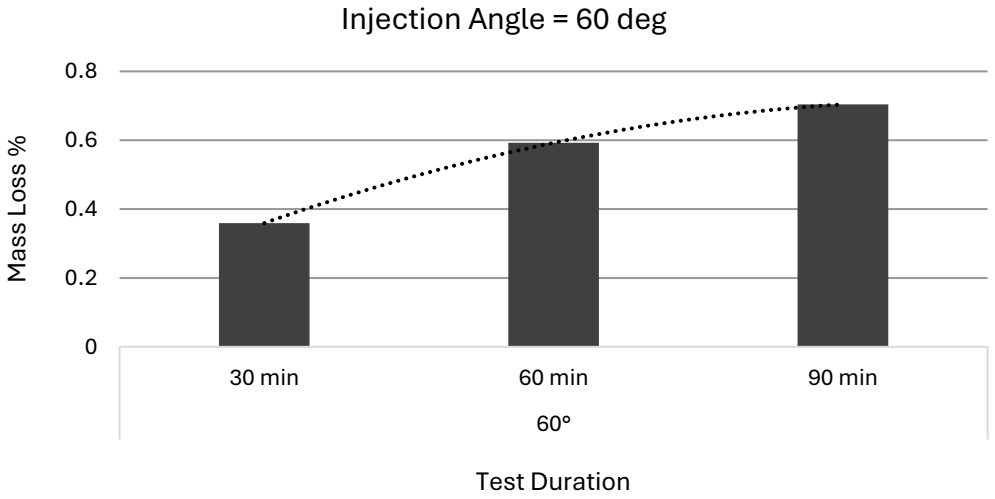

Figure 17 Erosion-induced mass loss of FR4-GFRC sample in different test durations, 45° impingement angle, 100 – 150µm sand size, and 12.5 m/s impingement velocity.

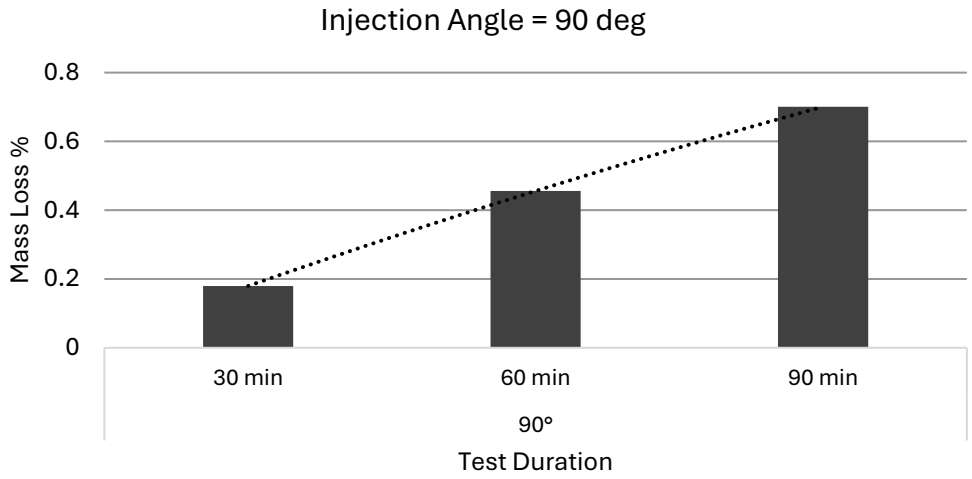

Figure 18 Erosion-induced mass loss of FR4-GFRC sample in different test durations, 90° impingement angle, 100 – 150μm sand size, and 12.5 m/s impingement velocity.

Discussion

Tidal turbines, as one of the most popular marine energy converters, will play a significant role in the renewable energy industry in the future, specifically in regions with high tidal ranges. These regions comprise rivers, channels, bays, and seabed. Any energy-converting facilities in such an environment confront peripheral impacts and marine wildlife interactions. For instance, a tidal turbine blade will experience micro to macro collisions with sand particles, animals, rocks, sunk tools, etc. These conflicts lead to structural integrity reduction on the surface at first. Gradually, this structural breakdown changes the external shape of the body. Surface modification can be rooted in different origins. For example, in the case of fibre-reinforced polymer (FRP) tidal turbine blades, a slight defect in fibre lay-up and manufacturing progress can lead to local concavities along the surface. On the other hand, some impacts cause scratches or erosion, which can appear as surface roughness. Starting with small pits at the blade's leading edge, erosion eventually reaches a critical level, with a considerable part of the blade surface being delaminated. Erosion, at the same time, can trigger other structural failures like fatigue, corrosion, ageing, biofouling, and impact-induced damages. All mentioned failures can be triggered or amplified due to a lack of structural integrity caused by erosion. Although there are mutual interactions between erosion and other failure modes, the influence of erosion on the rest is highlighted in this study. This emphasises the importance of accurately investigating erosion impacts on tidal turbines.

Furthermore, erosion can diminish the performance of tidal turbines. Slightly or severely eroded blades show different hydrodynamic behaviour than intact blades. This altered hydrodynamic response means different hydrodynamic efficiency. In other words, a structural phenomenon directly affects the turbine's power output. It should be noted that this stage of erosion is before the structural breakdown of the turbine, and it keeps operating but with less output. So, the hydrodynamic lifetime of the turbine can be significantly less than its structural endurance. It is crucial to know the optimum life span of a turbine during which the performance can stay cost-effective. So, we must know how much the performance would drop against erosion—knowing that the design can be modified to increase the structural strength. The operational conditions can be improved, as well, to differ the major efficiency

reduction. The question is how erosion solely influences the tidal turbine performance. The erosion behaviour and its effect on tidal turbine blades must be studied to find the answer. Erosion behaviour and its influence on hydrodynamic efficiency have been examined, starting with a flat plate. The results emphasise the importance of erosion, not only from the structural point of view but also from the hydrodynamic side of design.

As the experimental study in this research proves, the roughness profile on the FR4 GFRC, due to sand-salt-water erosion, is w-shaped, as shown in Figure 19.

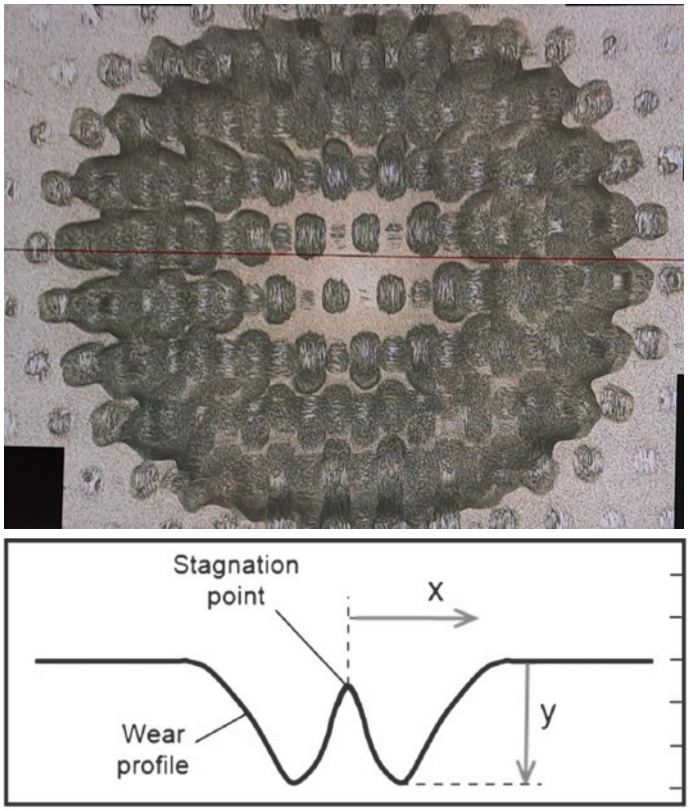

Figure 19 Sand-salt-water erosion-induced roughness profile on the FR4 GFRC surface, 90° impingement angle, 12.5 m/s injection velocity.

This is because of the stagnation point at the centreline of the impingement, where the flow velocity gets to zero and changes direction through the surface. This phenomenon is simulated using the previously used CFD tool, Star CCM+. Figure 20 clearly explains what happens at the stagnation point. The reason for less thickness reduction is the reduced flow (impact) velocity on the surface at the centreline of injection.

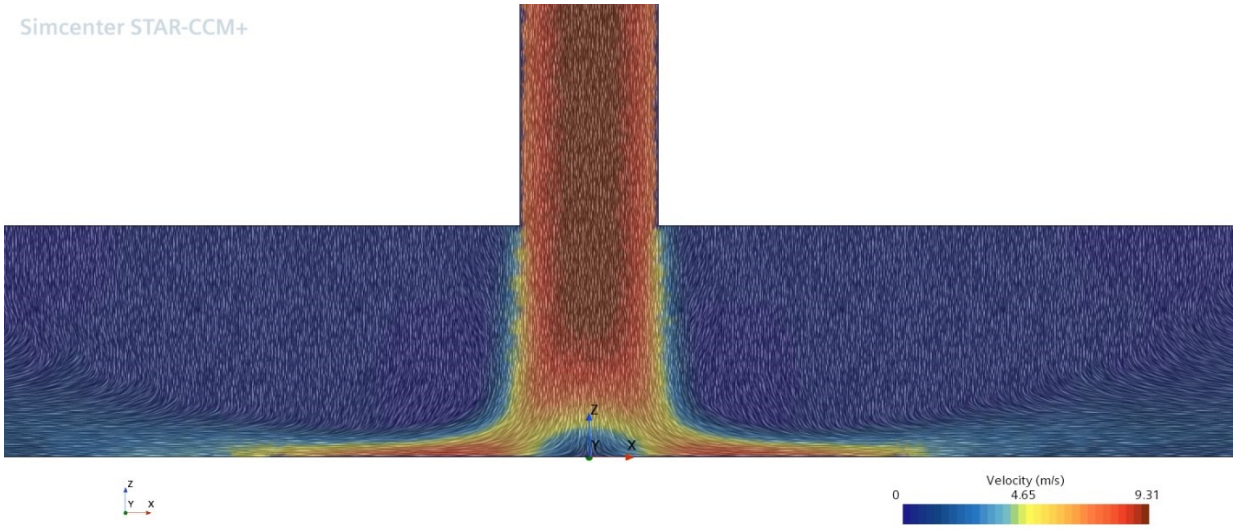

Figure 20 Velocity field in erosion rig test condition

Conclusion

Structural failures targeting structural integrity are a serious threat to any engineering design. These issues can require extra attention when dealing with underwater operational environments due to difficult accessibility and expensive maintenance and repair progress. Moreover, some marine-exclusive failures, like biofouling and sand-salt-water erosion, are on top of the others, like fatigue and corrosion. This makes it complex to monitor and analyse the sole effect of each failure. In this research, we studied the impact of early-stage erosion on the efficiency of the tidal turbine blade section. A tidal turbine hydrofoil, NACA 63-415, was simulated at Re = 1.6e+6, with different roughness heights, 0.01 mm to 1.2 mm, to replicate the early-stage erosion condition. In addition, the behaviour of FR4 GFRC (as a strong candidate for tidal turbine blades) against sand-salt-water erosion was experimentally investigated. FR4 samples were tested in a sand-salt-water erosion rig in impingement angles of $30°$, $45°$, $60°$, and $90°$, with the injection velocity of 12.5 m/s for 30, 60, and 90 minutes.

According to the numerical analysis, the efficiency constantly drops between the roughness height of 0.02 mm and 0.7 mm by up to 40 per cent. On the other hand, the experimental results show an increasing pattern of erosion against time. In addition, the role of impingement angle on the final mass loss was observed. The maximum mass loss in any test time duration happened at $60°$.

Future Works

As mentioned, this study is the first part of a two-part research. In the current part, we concentrated on the effect of erosion on the tidal turbine blade efficiency and the behaviour of FR4 GFRC against erosion numerically and experimentally. In the second part, we will investigate the different erosion distributions on the hydrofoil surface to concentrate on the blade leading-edge zone. Studying the impact of leading-edge erosion on tidal turbine blade efficiency leads us to find the most sensitive and effective parts of the blade in terms of erosion and hydrodynamic performance. This would help researchers and designers to improve the blade section design

structurally and hydrodynamically. In other words, optimising the operational condition and locally strengthening the blade can delay the early-stage erosion and huge performance drop.

References

Arcos, F.Z.d. (2021) *Hydrodynamics of highly-loaded axial flow tidal rotors*. Doctor of Philosophy Oxford.

Bak, C. *et al.* (2000) 'Wind tunnel tests of the NACA 63-415 and a modified NACA 63-415 airfoil'.

Clark, C.E. and DuPont, B. (2018) 'Reliability-based design optimization in offshore renewable energy systems'. *Renewable and Sustainable Energy Reviews,* 97 390-400.

Finkl, C.W. and Charlier, R. (2009) 'Electrical power generation from ocean currents in the Straits of Florida: Some environmental considerations'. *Renewable and Sustainable Energy Reviews,* 13 (9), pp. 2597-2604.

Groucott, S. *et al.* (2021) 'A study of raindrop impacts on a wind turbine material: Velocity and impact angle effects on erosion maps at various exposure times'. *Lubricants,* 9 (6), pp. 60.

Izadi Gonabadi, H. (2019) *Performance of low cost composites for tidal turbine applications*. Newcastle University.

Jing, F.-m. *et al.* (2017) 'Experimental study of hydrodynamic performance of full-scale horizontal axis tidal current turbine'. *Journal of Hydrodynamics, Ser. B,* 29 (1), pp. 109-117. https://doi.org/https://doi.org/10.1016/S1001-6058(16)60722-9.

Karthik, S. and Amarendra, H. (2020) 'Slurry Jet Erosion Test Rig: A Review of Erosive Particles Induction Methods and Its Test Parameters'. *Journal of Bio-and Tribo-Corrosion,* 6 1-15.

Khan, M.J. *et al.* (2009) 'Hydrokinetic energy conversion systems and assessment of horizontal and vertical axis turbines for river and tidal applications: A technology status review'. *Applied energy,* 86 (10), pp. 1823-1835. https://doi.org/10.1016/j.apenergy.2009.02.017.

Neill, S.P. (2018) 'Fundamentals of ocean renewable energy : generating electricity from the sea. [internet resource]'.

Qian, P. *et al.* (2019) 'Review on configuration and control methods of tidal current turbines'. *Renewable & sustainable energy reviews,* 108 125-139. https://doi.org/10.1016/j.rser.2019.03.051.

Sangiuliano, S.J. (2017) 'Turning of the tides: Assessing the international implementation of tidal current turbines'. *RENEW SUST ENERG REV,* 80 971-989. https://doi.org/10.1016/j.rser.2017.05.045.

Shiekh Elsouk, M., Santa Cruz, A. and Guillou, S. (2018) 'Review on the characterization and selection of the advanced materials for tidal turbine blades'. *Proceedings of the 7th International Conference on Ocean Energy,* 2018. pp.12-14.

Song, S. *et al.* (2020) 'Prediction of the fouling penalty on the tidal turbine performance and development of its mitigation measures'. *Applied Energy,* 276 115498.

Wood, R.J.K. *et al.* (2010) 'Tribological design constraints of marine renewable energy systems'. *Proc. R. Soc. A,* 368 (1929), pp. 4807-4827. https://doi.org/10.1098/rsta.2010.0192.

Zhou, Z. *et al.* (2017) 'Developments in large marine current turbine technologies – A review'. *Renewable & sustainable energy reviews,* 71 852-858. https://doi.org/10.1016/j.rser.2016.12.113.